

Trans-cinnamaldehyde loaded chitosan based nanocapsules display antibacterial and antibiofilm effects against cavity-causing *Streptococcus mutans*

Ran Mu^{a,b}, Hanyi Zhang^a, Zhiyuan Zhang^a, Xinyue Li^a, Jiakuan Ji^b, Xinyue Wang^b, Yu Gu^c and Xiaofei Qin^a

^aSchool of Biological Engineering, Zhuhai Campus of Zunyi Medical University, Guangdong, China; ^bDepartment of Clinical Medicine, The Fifth Clinical Institute, Zhuhai Campus of Zunyi Medical University, Guangdong, China; ^cSchool of Stomatology, Zhuhai Campus of Zunyi Medical University, Guangdong, China

ABSTRACT

Background: Dental caries is a multifactorial disease, and the bacteria such as *Streptococcus mutans* (*S. mutans*) is one of the risk factors. The poor effect of existing anti-bacterial is mainly related to drug resistance, the short time of drug action, and biofilm formation.

Methods: To address this concern, we report here on the cinnamaldehyde (CA) loaded chitosan (CS) nanocapsules (CA@CS NC) sustained release CA for antibacterial treatment. The size, ζ -potential, and morphology were characterized. The antibacterial activities in vitro were studied by growth curve assay, pH drop assay, biofilm assay, and qRT-PCR. In addition, cytotoxicity assay, organ index, body weight, and histopathology results were analyzed to evaluate the safety and biocompatibility in a rat model.

Results: CA@CS NC can adsorb the bacterial membrane due to electronic interaction, releasing CA slowly for a long time. At the same time, it has reliable antibacterial activity against *S. mutans* and downregulated the expression levels of QS, virulence, biofilm, and adhesion genes. In addition, it greatly reduced the cytotoxicity of CA and significantly inhibited dental caries in rats without obvious toxicity.

Conclusion: Our results showed that CA@CS NC had antibacterial and antibiofilm effects on *S. mutans* and inhibit dental caries. Besides, it showed stronger efficacy and less toxicity, and was able to adsorb bacteria releasing CA slowly, providing a new nanomaterial solution for the treatment of dental caries.

ARTICLE HISTORY

Received 16 May 2023

Revised 07 July 2023

Accepted 26 July 2023

KEYWORDS






Streptococcus mutans; dental caries; chitosan; cinnamaldehyde; nanocapsules; antibacterial agents; antibiofilm

Introduction

Dental caries (tooth decay) is an oral disease characterized by the chronic and progressive destruction of teeth, and it is caused by multiple factors and seriously endangers the oral health of people all over the world [1]. And it is sometimes painless, which makes it easy for most people to ignore it. If dental caries spreads to the dental pulp, it will occasionally lead to serious systemic diseases such as severe opportunistic infection and sepsis [1,2]. According to available studies, more than 2.0 billion people worldwide suffer from dental caries, which imposes a significant economic burden [3–5]. Biofilms are generated by the dysregulation of oral microbiota homeostasis, host factors, diet, and other factors. It is a dynamic microbial community immersed in a self-produced extracellular matrix, of which the main component is extracellular polysaccharides, which can protect the biofilm from saliva and agents [1]. Therefore, the prevention of biofilm formation is essential for the prevention of several oral diseases, including dental caries. *Streptococcus mutans* (*S. mutans*) is one of the major

cariogenic bacteria in the oral cavity, and it forms most of the biofilm [6,7]. Moreover, bacterial quorum sensing (QS), and the mechanism by which bacteria regulate related genes expression in accordance with population density, further promotes biofilm and virulence production. All of these causes lead to further demineralization of the teeth, resulting in caries [8–10]. Traditional treatments suggest taking a certain amount of fluoride, but this may not fundamentally inhibit the growth of bacteria and biofilm formation in the oral cavity. In addition, inappropriate fluoride exposure may have adverse consequences in some high fluoride areas for certain special populations [11,12]. More and more research has focused on the role of microorganisms in the pathogenesis of caries, but oral bacterial resistance to newly developed antibacterial drugs is another concern. It is urgent to develop new drugs that inhibit bacterial QS and biofilm formation for antibacterial to prevent dental caries.

In recent years, nano-drug delivery systems have been widely used in various fields. Nanoparticles can be designed to stimulate the release of drugs in

CONTACT Yu Gu  gylookfish@zmu.edu.cn  School of Stomatology, Zhuhai Campus of Zunyi Medical University, Guangdong, China; Xiaofei Qin  qxf2019300426@zmu.edu.cn  School of Biological Engineering, Zhuhai Campus of Zunyi Medical University, Guangdong, China
 Supplemental data for this article can be accessed online at <https://doi.org/10.1080/20002297.2023.2243067>

© 2023 The Author(s). Published by Informa UK Limited, trading as Taylor & Francis Group.

This is an Open Access article distributed under the terms of the Creative Commons Attribution-NonCommercial License (<http://creativecommons.org/licenses/by-nc/4.0/>), which permits unrestricted non-commercial use, distribution, and reproduction in any medium, provided the original work is properly cited. The terms on which this article has been published allow the posting of the Accepted Manuscript in a repository by the author(s) or with their consent.

different situations so that drugs are not affected by pH, enzymes, and other factors. They have also been used in the field of the oral cavity, such as hydroxyapatite platform nanoparticles for repairing caries [13], silver nanoparticles (Ag NPs) or zinc oxide nanoparticles (ZnO NPs) for treating periodontitis and oral ulcer [14,15], the iron oxide particle-based system for treating caries [16], etc. However, the toxicity caused by their accumulation in other organs is still controversial. The off-target effect and toxicity of these nanoparticles need to be further studied and verified [17,18].

Chitosan (CS), a product of deacetylation of chitin, has the advantages of good biocompatibility, antibiosis, and promotion of enamel remineralization, and is declared by US FDA to be GRAS (Generally Recognized as Safe) [19,20]. Lots of studies have shown that CS can inhibit the formation and adhesion of dental plaque and biofilm. Its positive potential groups can disrupt the bacterial cell membrane, thereby effectively inhibiting bacterial growth [19,21]. CS has been widely used in skin hydrogels, mouthwashes, and toothpaste, showing excellent antibacterial effects and enamel protection [20]. On the other hand, more studies showed that chitosan-based nanoparticles have higher antibacterial performance than pure chitosan due to the increase of specific surface area, which has better adhesion and can play an important role in the prevention and treatment of dental caries [19,21,22]. Cinnamaldehyde (CA), as a natural extract, has anti-inflammatory and broad-spectrum antibacterial effects. It could be a potential anti-caries drug due to its strong effect of inhibiting *S. mutans* [23–26]. However, its application is limited due to its low water solubility. Therefore, multifunctional nanosystems with high-concentration CA loaded need to be designed to inhibit *S. mutans*, to achieve the purpose of preventing dental caries.

Herein, a novel anti-caries nanosystem was prepared by loading CA into CS-based nanocapsules (Scheme 1). Due to the oily core and sustained release properties, the CS NC can load more CA while reducing toxicity. The slow release of CA@CS NC not only inhibited the acid production and biofilm formation of bacteria but also down-regulated the QS system, exhibiting strong anti-caries activity through rat caries model, as demonstrated from both *in vitro* and *in vivo* studies.

Materials and methods

Materials

CA (Table S1) and CS were purchased from Macklin Biological Co., Ltd. (Shanghai, China), the average molecular weight of CS is 3.0×10^5 Da, and the degree of deacetylation is about 10%. Soy lecithin was purchased from Pengrui Biomedicine Co., Ltd.

(Pizhou, China). Hematoxylin and eosin (HE) dye solution, neutral gum, and CCK-8 kit were purchased from BioSharp Co., Ltd. (Hefei, China). Miglyol 812N was purchased from Beijing Fengli Jingqiu Pharmaceutical Co., Ltd. (Beijing, China). Phosphate buffered solution (PBS) solution was prepared with NaCl, KCl, Na_2HPO_4 , and KH_2PO_4 . The pH value of PBS was adjusted with hydrochloric acid and sodium hydroxide to 7.4, and the concentration of PBS is 0.1 M. The model strain of *S. mutans* (UA159) was donated by the stomatology laboratory of Zunyi Medical University, and human oral epithelial cells (HOECs) were derived from the cell-sharing platform of Zunyi Medical University. Sprague-Dawley rats were purchased from Zhuhai BesTest Bio-Tech Co., Ltd. (Zhuhai, China).

Preparation of nanocapsules and nanoemulsions

Chitosan-based nanocapsules and nanoemulsions were prepared according to previous methods with slight modifications [27,28]. The nanoemulsions (NE) were prepared using an identical protocol as for the CS NC, but the aqueous phase consisted only of deionized water. To prepare the CA loaded CS NC (CA@CS NC) and NE the protocol was identical as for the blank systems, but, 10 mM ethanolic CA stock was mixed with 10 mL ethanol and added in the organic phase.

Physicochemical characterization of nanomaterials

The ultrastructure of the nanomaterials was investigated by TEM using a RuliTEM (Hitachi, Japan). Add an appropriate amount of water in a ratio of 1:10 diluted nanocapsules and nanoemulsions, then use a Zetasizer NanoZS (Malvern, UK) equipped with 4 mW helium/neon laser ($\lambda = 633$ nm) and detection was at an angle of 173° to scan the size and ζ -potential determined by dynamic light scattering (DLS). In addition, ζ -potentials of 1:10 dilutions of CA@CS NC and *S. mutans* were measured. After that, the two were mixed 1:1 and measured the ζ -potential.

Measurement of encapsulation rate and cumulative release

To measure the prepared CA@CS NC, 6 mL suspension of the prepared nanocapsules after dialysis was transferred into a dialysis bag (1000 Da) and immersed into 300 mL PBS (pH = 7.4) at room temperature. Then 3 mL of the solution at varied time intervals were taken from the dialysates to measure the concentration of released CA by monitoring the absorption peak located at 280 nm by UV – Vis spectrometry. After the sampling solution was taken,

3 mL fresh PBS was added back to keep the total volume of the test solution constant.

Bacterial strain and growth curve assay

S. mutans (UA159) was grown in Brain Heart Infusion Broth (BHI) at 37°C. *S. mutans* (1×10^8 CFU/mL) cultured overnight to mid-log phase strain was added to a 96-well plate. To explore the effect of different components of CA@CS NC on bacterial growth, the final concentrations of groups corresponded to those of the CA@CS NC group. The concentration of CA and CS in the CA@CS NC group was 1 mM (132 µg/mL) and 100 µg/mL, respectively. Thus, CA was 1 mM in the CA group and CA@NE group, and CS was 100 µg/mL in the CS group and CS NC group. The NE did not contain CS and CA. To verify the effect of other potential components on bacteria, the dilution method of NE group was referred to CA@CS NC group, so that the concentration of components with potential antibacterial effects such as lecithin, Miglyol 812N, et al corresponded to CA@CS NC. In addition, kanamycin (KANA) was used as a positive control. The optical density at 600 nm (OD_{600}) was measured every 2 h throughout the incubation using a Multiskan SkyHigh (Thermo Scientific, USA). Every treatment was performed in duplicate in at least three different experiments.

Glycolytic pH drop assay

The effect on acid production by *S. mutans* was determined by the method of the previous study with an appropriately extended measurement time [26,29]. *S. mutans* were harvested in the mid-log phase, centrifuged (4°C, 5000 rpm, 5 min), and washed with saline solution (50 mM KCl +1 mM MgCl₂). Thereafter, CA@CS NC was added to BHI to a final concentration of 1 mM, and the remaining groups were added to a final concentration of 1% (w/v) glucose as in the above experiment, and the initial pH of the mixture was adjusted to about 7.3 with KOH. The pH reduction was monitored over an 8 h period. The results correspond to three experiments independently.

CLSM analysis

Biofilms were formed on circular glass slides in a 24-well plate. Specifically, *S. mutans* (UA159) in the logarithmic growth phase was adjusted to a final density of 2×10^6 CFU/mL with BHI medium supplemented with 1% sucrose. 12 h after biofilm formation, the circular glass slides were removed and placed in another new 24-well plate for treatment. The glass slides were washed three times (1 min/time) with PBS (pH = 7.4), and then CA@CS NC or other

drugs were added into corresponding wells. After 10 min treatment, the glass slides were washed three times with pH 7.4 PBS and then transferred into a new 24-well plate containing fresh BHI medium supplemented with 1% sucrose. This treatment regimen was administered every 12 h for a total of 3 times. Thereafter, LIVE/DEAD BacLight bacterial cells (OR, United States) containing SYTO 9 dye and propidium iodide were stained in the dark for 30 min for confocal laser scanning microscopy imaging (Leica, Germany).

CCK-8 assay

HOECs were cultured in high-glucose medium in an incubator at 37°C, 90% relative humidity, and 5% CO₂. First, the cultured cells were seeded onto 96-well plates for 24 h, 100 µL per well, and the cell density was about 5000 cells/well, and repeated three times. CA@CS NC and CA were added to different wells. After culturing for 6 h, 10 µL CCK-8 reagent was added, and the growth was continued for 12 h. The culture medium was washed with Hanks solution, and 200 µL high-glucose medium was added to measure the optical density of the solution at 450 nm (OD_{450}) with a Multiskan SkyHigh. The results correspond to three experiments independently.

RNA isolation and quantitative real-time PCR (qRT-PCR)

To study the effect of CA@CS NC on the expression of genes of *S. mutans*, we contrasted the effects of CA@CS NC and blank groups on the genes of *S. mutans* at equal concentrations. Among the genes studied (Table 1), there are 5 genes involved in QS regulation (*comB*, *comE*, *comS*, *comA* and *comR*), 1 gene involved in biosynthesis and adhesion (*gbpB*), 1 gene involved in two-component signal transduction system and bacterial virulence (*vicR*), 3 genes involved in extracellular polysaccharide synthesis (*gtfB*, *gtfC*, *gtfD*) [26,30–33]. The organism was treated with CA@CS NC and cultured in medium for 12 h. Cells were harvested by centrifugation from 15 mL centrifuge tube and then incubated by lysozyme (20 mg/mL) at 37°C for 25 min. Total RNA was extracted from cells using Trizol reagent (Solarbio, China) according to the manufacturer's instructions. Purified RNA was dissolved in 30 µL of DEPC-treated water and stored at –80°C until required for cDNA labeling. cDNA was generated with HiScript III RT SuperMix for qPCR (+gDNA wiper) (Vazyme, R323–01). The cDNA samples were stored at –20°C until used.

The qRT-PCR analysis was carried out in 96 well plates. Reaction mixture: in a total volume of 10 µL, consisted 5 µL 2X SYBR Green PCR Master Mix, forward and reverse primers (0.2 µL each), 3.6 µL ddH₂O

Table 1. Nucleotide sequences of primers used in qRT-PCR and based on *S. mutans* genome database (NCBI).

Gene	Description	Primer sequence (5'–3')
<i>16S rRNA</i>	Normalizing internal standard	F: CCTACGGGAGGCAGCAGTAGR: CAACAGAGCTTTACGATCCGAAA R: CAACAGAGCTTTACGATCCGAAA
<i>comB</i>	Putative ComB	F: CCACTCAAACCGTCAGACTR: GCTGCTTTCCTTGCTTTTCG R: GCTGCTTTCCTTGCTTTTCG
<i>comE</i>	Response regulator of the competence regulon	F: GCCCTTTTCAGGGATAGCGTR: AGGACGTCTTGAACCACCA R: AGGACGTCTTGAACCACCA
<i>comS</i>	Regulator of genetic competence ComS	F: TTTTGATGGGTCTTGACTGGR: TTTATTACTGTGCCGTGTTAGC R: TTTATTACTGTGCCGTGTTAGC
<i>comA</i>	Two-component response quorum-sensing regulator	F: ACGAGCCTAACAAGGGGATTR: CCCTGAGGCATTTGTTCAAT R: CCCTGAGGCATTTGTTCAAT
<i>comR</i>	TetR family copper-responsive transcriptional repressor ComR	F: CGTTTAGGAGTGACGCTTGGR: TGTGGTCCGCATAGGTTG R: TGTGGTCCGCATAGGTTG
<i>gbpB</i>	Glucan binding protein	F: ATGGCGGTTATGGACACGTR: TTTGGCCACCTTGAACACCT R: TTTGGCCACCTTGAACACCT
<i>vicR</i>	Response regulator	F: TGACACGATTACAGCCTTTGATGR: CGTCTAGTTCTGGTAACATTAAGTCCAATA R: CGTCTAGTTCTGGTAACATTAAGTCCAATA
<i>gtfB</i>	Accessory Sec system glycosylation chaperone GtfB	F: GGACAGCCGATGATTTGGR: CTTGCTTGACAGCTCCTC R: CTTGCTTGACAGCTCCTC
<i>gtfC</i>	Glucosyltransferase GtfC	F: CCATCGAAACCCTGCTTAAAR: GCGATCAGAAGCCTTCAAAC R: GCGATCAGAAGCCTTCAAAC
<i>gtfD</i>	Glucosyltransferase-S	F: AACCGCACCAACCAGTR: CAACGGCATCAACACGAA R: CAACGGCATCAACACGAA

O and 1 μ L 10X diluted cDNA. Reaction procedure: the PCR conditions included an initial denaturation at 95°C for 5 min; followed by 40 cycles of denaturation at 95°C for 10 s, annealing (60°C for 20 s), extension (72°C for 1 min). The relative gene expression was analyzed using the $2^{-\Delta\Delta C_t}$ method. The results correspond to three experiments independently.

Rat caries model

The animal study was approved by the Laboratory Animal Welfare and Ethics Committee of Zunyi Medical University (ZMU21-2302-008). The rat caries model was performed using a modified method [34,35] (Scheme 2). We determined the optimal sample size of animals used based on the literature [36]. Forty of 21-day-old male SD rats were fed with diets containing carbenicillin, ampicillin, and chloramphenicol from 21 to 24 day-old before establishing oral bacterial inoculation. After 3 days, the rats were inoculated twice daily with *S. mutans* suspension from 24 to 29 day-old. At the same time, these rats were fed Keyes 2000 # diet until the end of the experimental period to induce severe dental caries. After the completion of bacterial solution inoculation, rats were anesthetized with isoflurane every 3 days and fed with 200 μ L of the corresponding drug in each group, and the drug was dipped into a sterile cotton swab and fully smeared on the tooth surface of rats for 5 min. Moreover, general conditions such as body weight, fur color, and activity of the rats were recorded throughout the experiment. Finally, the rats were sacrificed after gas anesthesia at 45 day-olds.

Rat organ index and HE staining

The organ index method can reflect whether there is a change in organ volume and weight through the

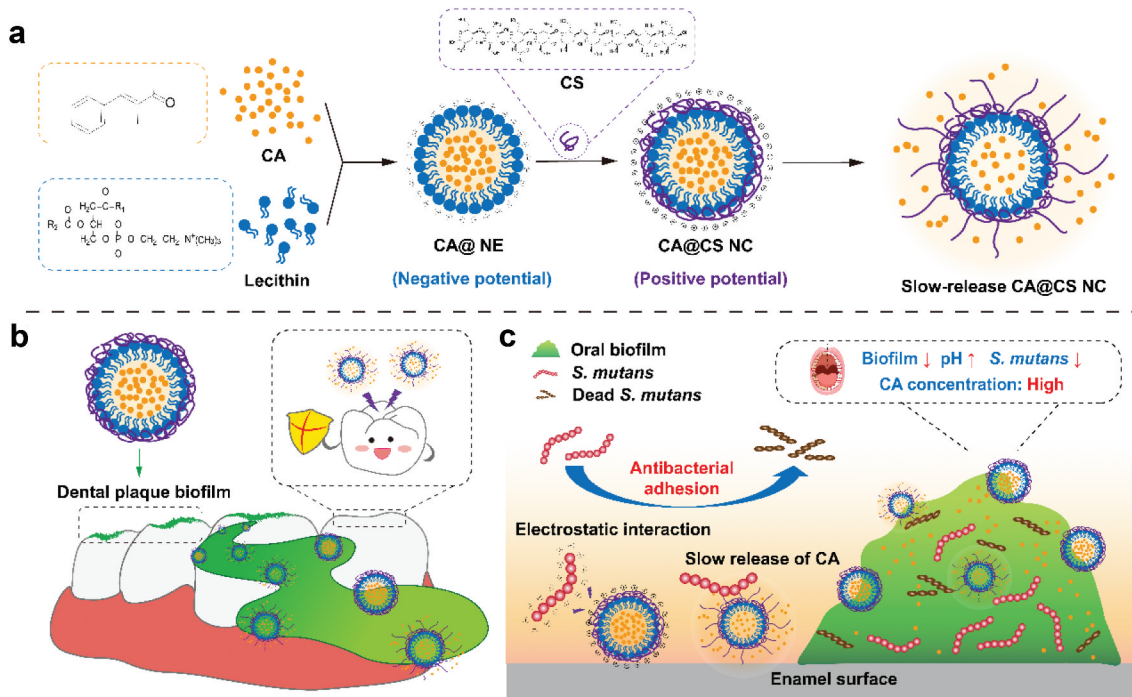
proportion of body weight in the body, which can roughly show the toxicity of drugs to different organs [37,38]. The total body weight of the rats was weighed and recorded before dissection. The heart, liver, spleen, lung, kidney, and testis were obtained by dissection, weighed, and recorded. Organ index = (organ weight/total body weight) \times 100%. Then, the main organs collected were then stained with HE and observed under a microscope.

Evaluation of dental plaque and caries severity in rats

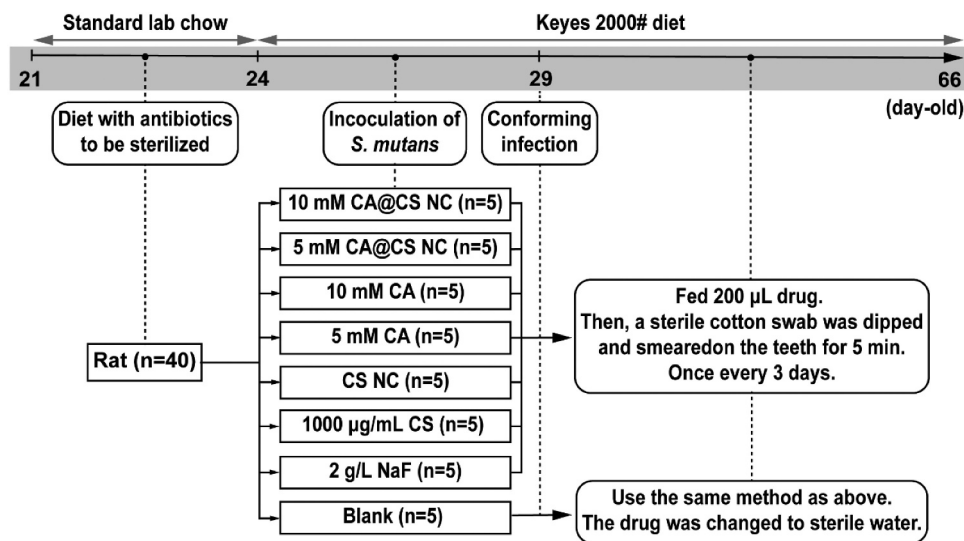
After decapitation, the jaw bone was observed under a stereomicroscope, and the dental plaque was quantitatively evaluated using the method of Shuhei Naka *et al* [39]. Then the skull was removed and placed in an autoclave at 121°C for 15 min. The attached soft tissue was peeled off with a scalpel, and the jaw was cleaned and dried at room temperature. All of the specimens were immersed in a 0.4% ammonium purpurate staining solution for 12 h, rinsed, and semi-sectioned along the occlusal surfaces of maxillary and mandibular molars using a diamond cutter (thickness: 0.1 mm). Caries on the rat molars were observed and evaluated under a stereomicroscope according to the caries diagnosis and scoring method reported by Keyes [39–41].

Statistical analysis

All data were expressed as mean \pm standard deviation. Two-way analysis of variance (ANOVA) with the Geisser-Greenhouse correction and Tukey's multiple comparisons test, one-way ANOVA, and Holm-Sidak's multiple comparisons test were used to



Scheme 1.(a) CA@CS NC has a positively potential surface and continuously releases CA. (b) CA@CS NC can inhibit dental plaque to protect teeth. (c) At the same time, it can adsorb *S. mutans* through electrostatic interaction and slowly release CA, thereby inhibiting bacterial growth, acid production, biofilm formation and other risk factors leading to dental caries.



Scheme 2.The scheme design of this study. To evaluate the anti-carries effects of nanomaterials and related drugs in a modified caries rat model.

calculate the significance of differences between groups under test conditions (GraphPad Prism 8.4.0 software, United States).

Results

Nanocapsules exhibit unique physical properties and adsorb *S. mutans*

Firstly, Figure 1(d) shows the nanomaterials-related structures and abbreviations, which will be used to replace nanomaterials in the results. And the ζ -

potential refers to the potential of the shear plane, also known as Zeta potential, which is an important index to characterize the stability of colloidal dispersions. Polymer dispersity index (PDI) is a measure of the heterogeneity of sizes of molecules or particles in a mixture [42]. Table 2 shows the sizes and ζ -potential of nanocapsules and nanoemulsions. The results showed that the prepared nanomaterials were homogeneous (PDI < 0.2). And the size is mostly in the range of 210 ~ 250 nm with obvious positive potential. Figure 1(a) shows the TEM image of CS NC, which has a spherical morphology and a core-shell structure

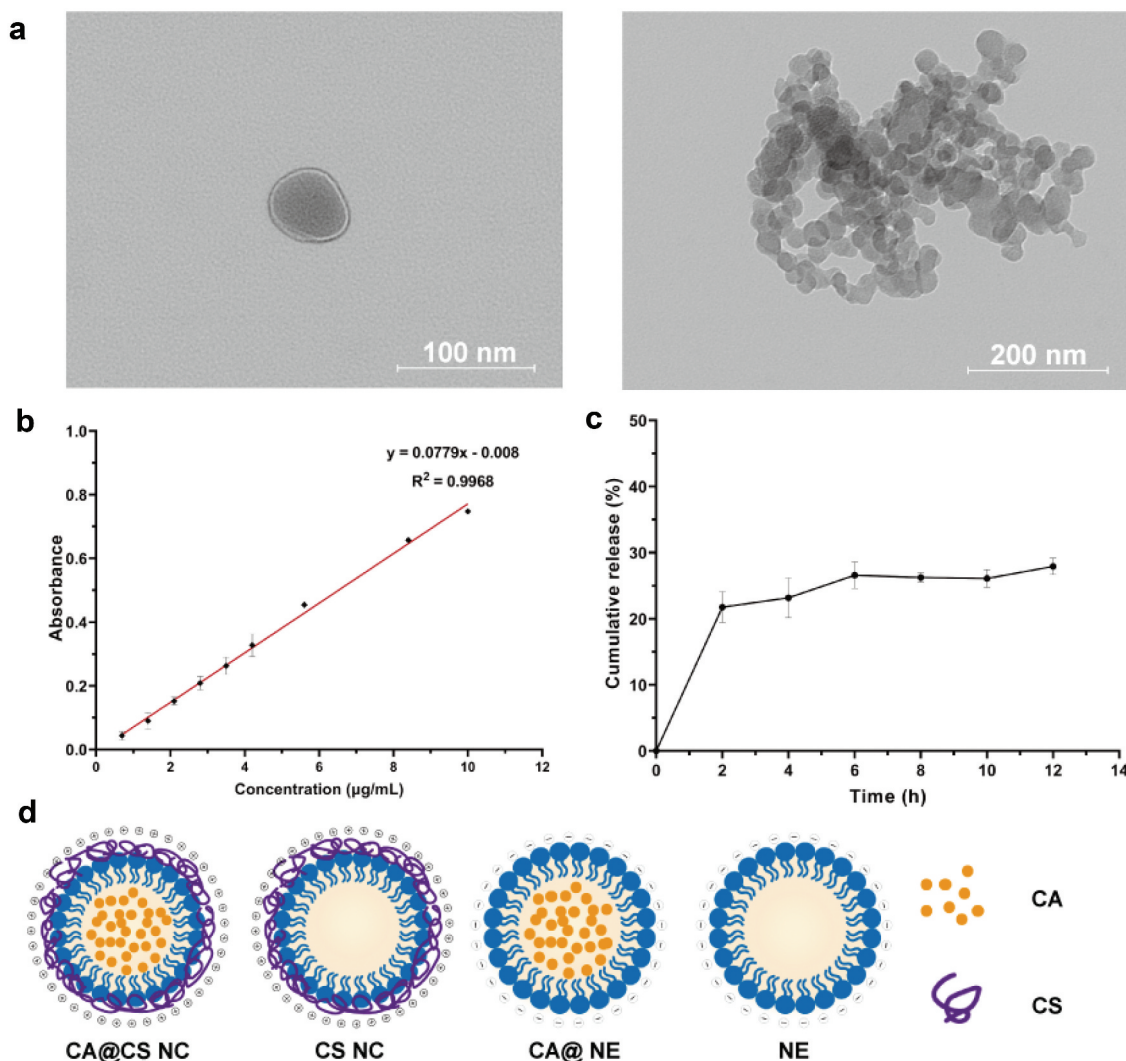


Figure 1. (a) Representative TEM images of CS NC. (b) The CA concentration standard curve. (c) The cumulative release of 10 mM CA@CS NC. (d) Schematic representation of the nanomaterials and related agents with abbreviations.

with a particle size of about 150 nm. The larger size measured by DLS is due to solvent effects in the hydrated state. On the other hand, nanoemulsions have a particle size slightly smaller than nanocapsules, mostly around 200 nm, and exhibit clear negative potential. And nanoemulsions are smaller than nanocapsules because of the lack of CS shell. These characteristics are similar to previous studies [27,43,44]. The bacteria showed negative potential, however, when *S. mutans* was mixed with CA@CS NC, the bacteria

solution showed positive potential when combined with nanocapsules, indicating the electronic interaction between *S. mutans* and nanocapsules [45,46]. In addition, Figure 1(b) shows the calibration curve of CA, $y = 0.0779x - 0.008$ ($R^2 = 0.9968$). Based on this curve, the encapsulation rates of 5 mM and 10 mM CA@CS NC were 81.74% and 90.59%, respectively. And Figure 1(c) shows the sustained release of 10 mM CA@CS NC, which has a slower release rate of 21.7% in the first 2 h and 27.9% in the first 12 h.

Table 2. Size and ζ -potential of nanomaterials and *S. mutans*. And the changes of 5 mM CA@CS NC bound with *S. mutans*.

Group	Size (d. nm)	PDI	ζ -potential (mV)
10 mM CA@CS NC	215.1 ± 6.6	.103 ± .016	35.0 ± .643
5 mM CA@CS NC	211.2 ± 3.3	.046 ± .038	23.0 ± 1.447
NC	239.3 ± 4.7	.104 ± .070	19.0 ± .700
10 mM CA@ NE	183.4 ± 3.3	.131 ± .020	-26.6 ± 1.217
5 mM CA@ NE	204.3 ± 2.5	.138 ± .019	-28.1 ± 1.290
NE	208.8 ± 2.5	.138 ± .047	-25.6 ± .252
<i>S. mutans</i>	1487.0 ± 114.9	.244 ± .015	-6.9 ± 1.721
5 mM CA@CS NC + <i>S. mutans</i>	762.3 ± 70.4	.246 ± .020	12.7 ± .981

CA@CS NC can effectively inhibit the growth and biofilm formation of *S. mutans*, down-regulate the expression of related genes

Figure 2(a) shows the growth inhibition of *S. mutans* by the nanomaterials and the related drugs. According to the result in Figure S1, the Minimum Inhibitory Concentration (MIC) of CA against *S. mutans* UA159 was 500 µg/mL (about 3.7 mM), which was much higher than the concentration (1 mM) set in this study. After 12 h of bacterial culture, 1 mM CA@CS NC ($OD_{600} = 0.198 (\pm 0.035)$) significantly inhibited the bacteria, and the inhibitory effect was better than that of 1 mM CA ($OD_{600} = 0.469 (\pm 0.009)$). According to the results in Figure 1, CA@CS NC can sustained-release about 30% CA (0.3 mM) within 12 hours at a concentration below 1 mM CA. In the comparison of OD_{600} values, CA@CS NC showed a better effect than CA at lower concentrations. At the same time, it was found that floccule was formed after the addition of nanocapsules. Therefore, we carried out

microbiological turbidimetry and the results (Figure S2) also showed that CA@CS NC showed better effects than CA.

Dental demineralization caused by acid production by bacteria such as *S. mutans* is an important factor leading to caries. Inhibition of acid production by cariogenic bacteria such as *S. mutans* can prevent caries. Figure 2(b) shows the effect of the drugs on acid production by *S. mutans*. According to the above results, the sustained release of CA@CS NC was approximately 30% within 8 hours. At this time, the effective CA concentration in the CA@CS NC group was approximately 0.3 mM. Compared with the pH value of the blank group ($4.200 \pm (0.010)$), the acid production of bacteria in the other drug treatment groups was inhibited except NE ($4.263 \pm (0.015)$). In summary, CA@CS NC exerted a similar effect as 1 mM CA with a sustained release of 0.3 mM CA concentration. In addition, CS also inhibited acid production, suggesting a synergistic effect of CA@CS NC on the inhibition of acid production in *S. mutans*.

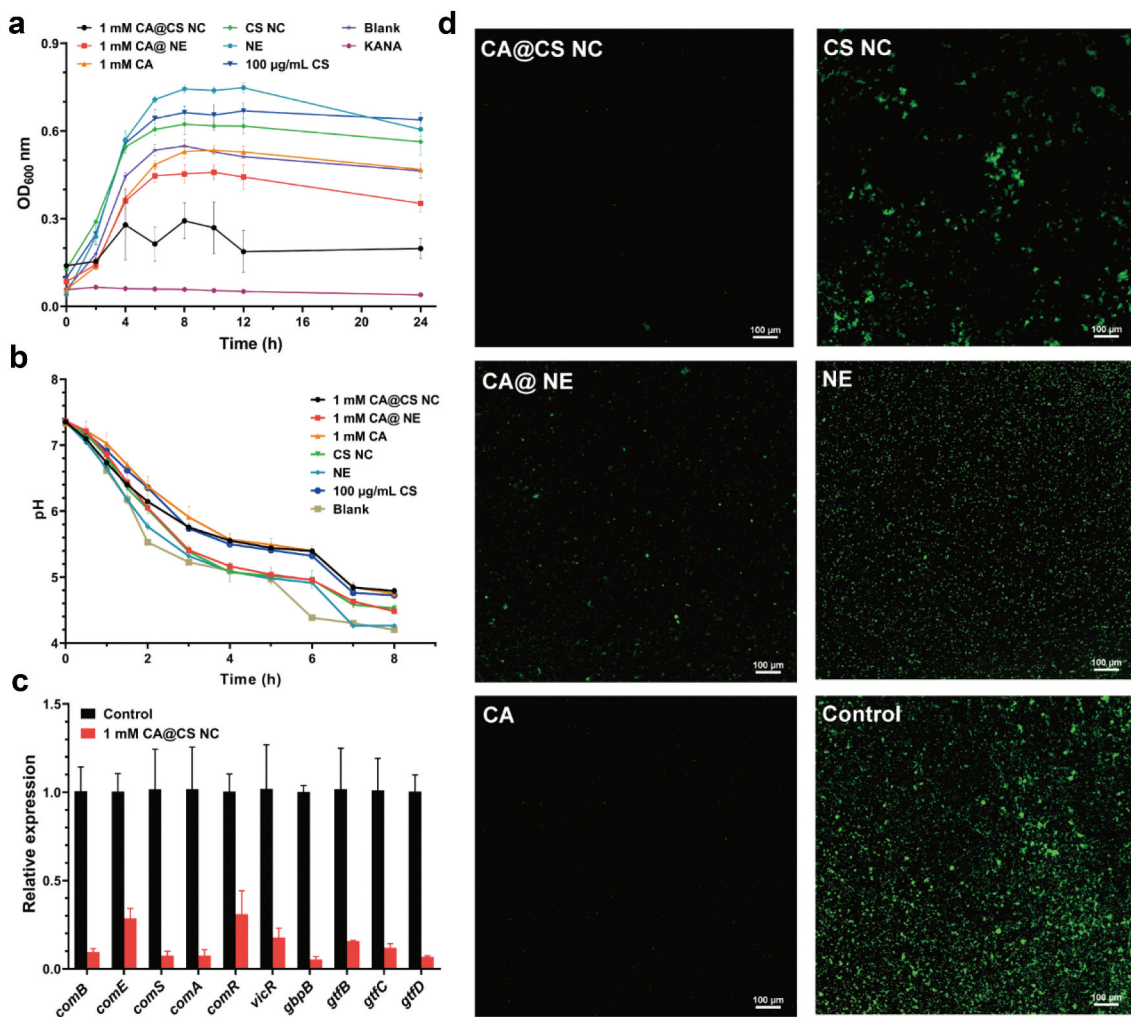


Figure 2.(a) Effects of composition of different drugs on the growth curve of *S. mutans*. (b) Effect of different drugs on acid production. (c) 1 mM CA@CS NC regulate the expression of genes related to *S. mutans*. (d) Inhibitory effect of different drugs components on biofilms of *S. mutans*.

To understand the expression of genes related to QS, virulence, biofilm and adhesion of *S. mutans*, the effect of CA@CS NC on *S. mutans* was quantitatively studied by qRT-PCR. The results in Figure 2(c) showed that the CA@CS NC successfully down-regulated QS, virulence, adhesion, biofilm-related, and extracellular polysaccharide synthesis gene expressions.

Figure 2(d) shows visually the inhibitory effect of nanomaterials and CA on the biofilm formation of *S. mutans* by CLSM assay. As can be seen from the results of the nanomaterials, a comparison between nanocapsules and nanoemulsions, the electrostatic interaction of nanocapsules plays an important role in significantly inhibiting biofilm formation by bacterial aggregation. In addition, the biofilm formation was strongly inhibited by CA loaded nanomaterials compared with the unloaded nanomaterials. In conclusion, CA@CS NC could absorb *S. mutans* and slow release of CA, significantly inhibit biofilm formation through the combination of CS and CA.

The nanocapsules showed no obvious toxicity *in vivo* and *in vitro*

Figure 3(a) shows the cytotoxicity of CA@CS NC and CA to HOECs by CCK-8 assay. The results showed that the cytotoxicity of CA@CS NC was significantly lower than that of CA at same concentration. When the concentration of CA@CS NC was 0.25 mM, the cell survival rate was 102.703 (± 23.682)%, while the cell survival rate of the same concentration of CA was only 60.566 (± 19.382)%. The above results showed that the slow release of CA from CA@CS NC reduced the cytotoxicity.

In the rat model, we weighed the rats and recorded fur color, diet, and activity. During the experiment, the rats were generally in good condition, and there was no significant difference in body weight among the groups (Figure 3(b)). In addition, organs were weighed after sacrifice, and there was no significant difference in organ index ($P > 0.05$) as shown in Figure 3(c) too. In this study, drugs were

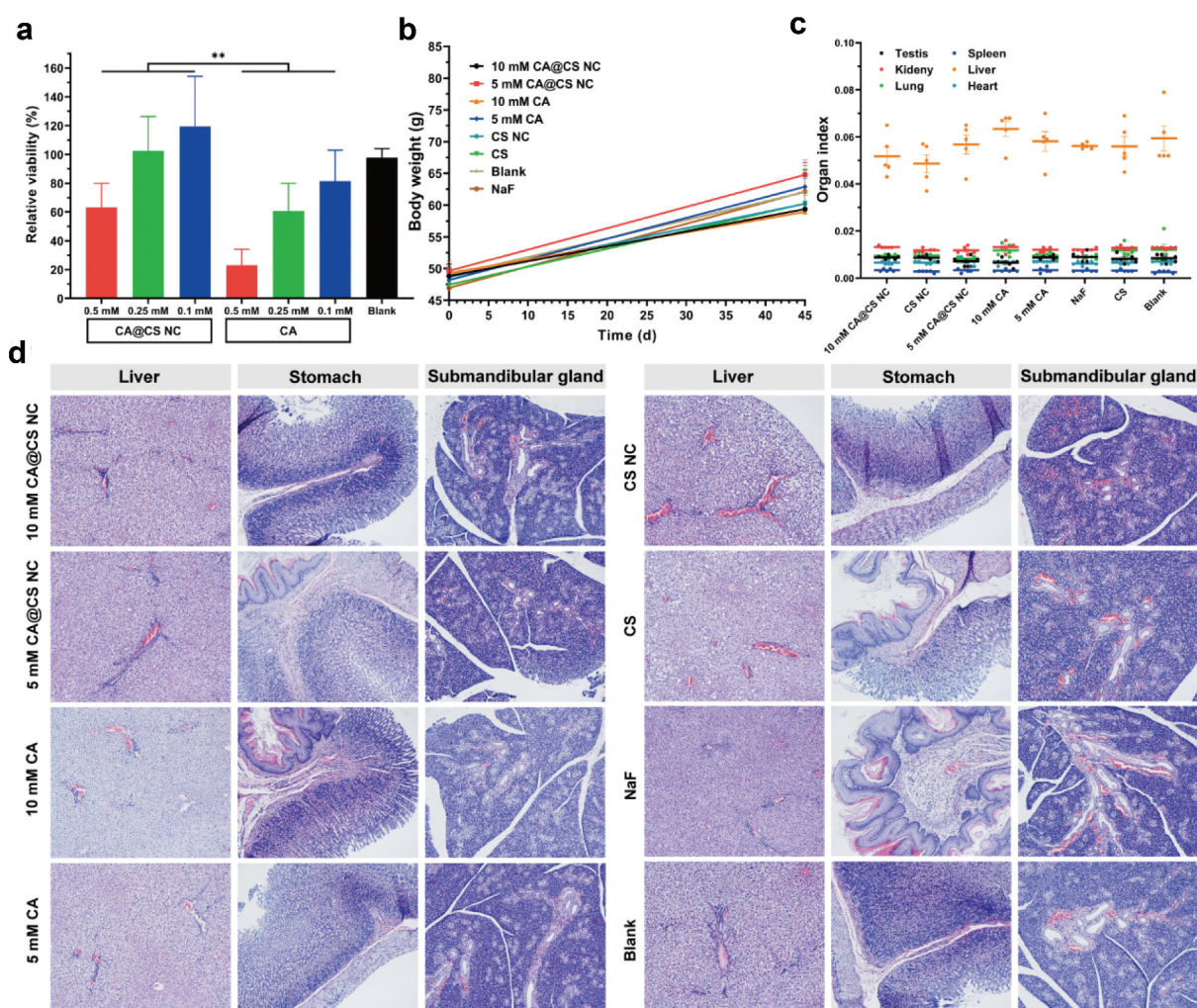


Figure 3.(a) *In vitro* cytotoxicity assay of CA@CS NC and CA. (b) Rat body weight changes and (c) Organ index in the rat model. (d) HE stained sections of rat liver, stomach and submandibular gland.

administered by smearing on the teeth and did not enter the bloodstream. To evaluate the condition of the organs, we prepared pathological HE stained sections of potentially damaged organs. From the results in Figure 3(d), the pathological specimens of liver, stomach, and submandibular gland showed a small amount of inflammatory cells infiltrate the tissue, and there was no obvious organ damage which could be observed.

CA@CS NC showed excellent inhibition of dental plaque and caries in the rat model

Due to the antibacterial, acidogenic, and anti-biofilm formation effects of CA@CS NC *in vitro*, we further evaluated its anti-caries effect in a rat model. Figure 4(a) shows the dental plaque and caries (sulcal lesions) of the rats; macroscopic observation showed that the CA@CS NC group had significantly reduced plaque, and its plaque was similar to that of the NaF group. According to the results of tooth section staining, the teeth in the CA@CS NC and NaF groups showed lighter coloration after staining, indicating that *S. mutans* could cause initial lesions after drug treatment. However, other groups showed dark red or reddish-brown colorations, indicating moderate or even severe lesions.

To further comprehensively evaluate the caries, we evaluated the dental plaque (Figure 4(b)) and caries lesions results (Figure 4(c,d)) by plaque score and Keyes' score, respectively. As shown in Figure 4(b), the score of CA@CS NC group (1.700 (±0.326)) was similar to that of NaF group (1.800 (±0.371)), which showed significant less plaque compared with other drug treatment groups.

According to the depth of caries, the caries classification was divided into different lesions (E, Ds, Dm, and Dx). Due to the strong cariogenic ability of the modified rat model, a large number of superficial caries were produced in each group, and the anti-caries effect was not obvious among the drug treatment groups. However, for moderate and severe lesions (Ds, Dm, and Dx), significant differences were observed among groups. Figure 4(c) compared the caries lesions of CA@CS NC and CA, and it can be seen that the effect of CA@CS NC group in inhibiting Ds, Dm and Dx lesions was significantly better than that of the CA group. On the other hand, Figure 4(d) shows the caries lesions of the nanocapsules with different CA concentrations. With the increasing concentration of CA, it showed excellent anti-caries performance. In addition, there was no significant difference ($P > 0.05$) between the CS NC group and the blank group, and the 5 mM CA and CS had poor anti-caries effect (Figure S3).

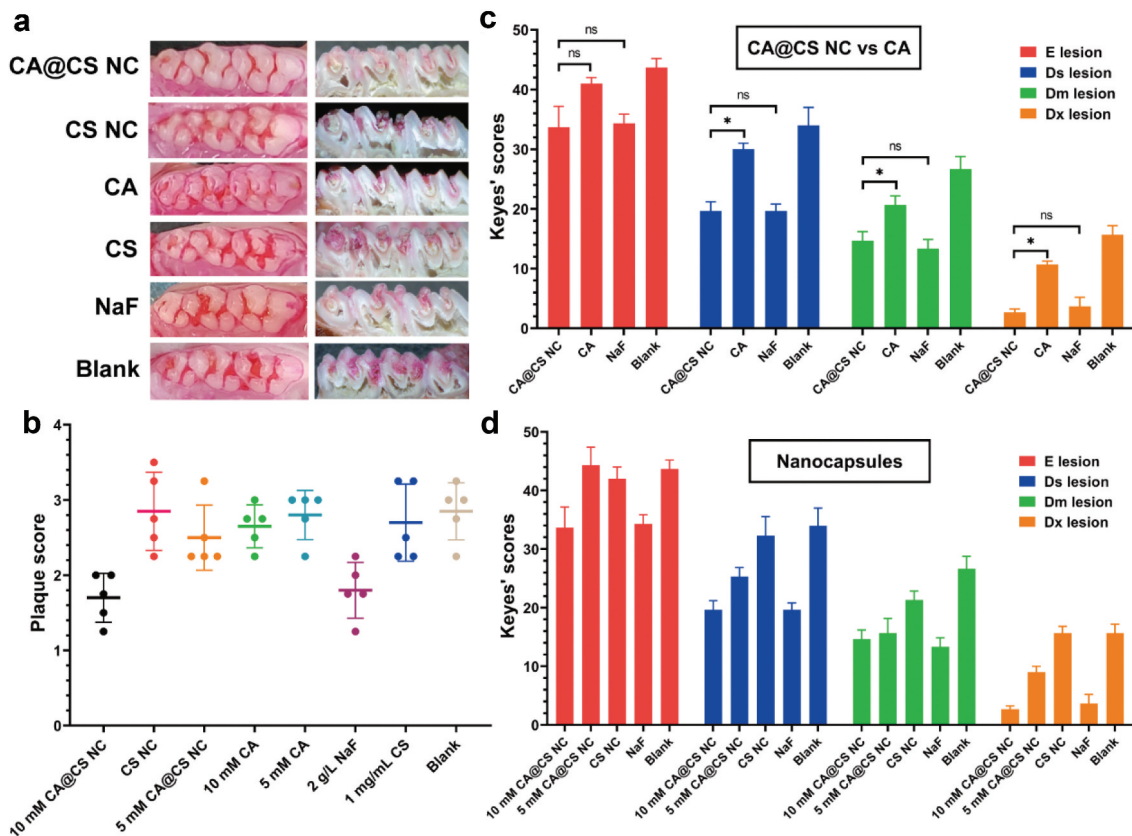


Figure 4.(a) the smooth surface of the tooth after plaque staining, and the section of the tooth after Keyes score staining. (b) Dental plaque staining in rats. (c) Comparison of the lesion of caries between CA@CS NC and CA (d) Effect of CA concentration in the nanocapsules system on Keyes' scores.

Discussion

The chitosan-based nanocapsules have an oil core with a size of 210 ~ 250 nm which can improve the problem of weak antibacterial effect of fat-soluble drugs caused by poor water solubility [47]. And they have CS shells with positive potential, which can adsorb bacteria through electrostatic interaction. At the same time, the loaded fat-soluble drugs can be slowly released by the mechanism of natural leakage, and the antibacterial effect can be stronger for a long time. As a biocompatible drug, chitosan-based nanocapsules have been widely used for antibacterial and anti-tumor [48–50]. For example, Capsaicin@chitosan nanocapsules (CAP@CS NC) can inhibit *Escherichia coli* and *Staphylococcus aureus* by encapsulating capsaicin. In terms of anti-tumor, curcumin loaded chitosan/perfluorohexane (CS/PFH) nanocapsules (CS/PFH-CUR-NCs) were used to treat rectal cancer by oral administration [51–53]. Thus, chitosan-based nanocapsules have great potential to combat chronic infectious diseases.

Dental caries is a multifactorial oral disease, and *S. mutans* and other bacteria play an important role in the occurrence of dental caries. *S. mutans* mainly adheres to the tooth surface to form biofilm, produce acid, and exert QS effect, which is a key factor leading to caries [54–56]. In the study, we chose a concentration below the MIC of CA (500 µg/mL). At the concentration of 1 mM (132 µg/mL), the growth of *S. mutans* could not be effectively inhibited by CA alone, reflecting the antibacterial property of low concentration of CA@CS NC. The positively potential CS shells adsorbed bacteria and slowly released CA, forming a relatively high concentration of CA around bacteria, inhibiting acid production and biofilm formation, and down-regulating the expression of related genes of *S. mutans*. As mentioned above, acid production is an important factor in the occurrence of dental caries. Based on the sustained release assay of CA@CS NC, only about 30% CA was released within 8 h. And the results of the glycolytic pH drop assay showed that CA@CS NC and CA had similar effects within 8 h, at which time the CA in CA@CS NC was not completely released. These results indicate that CA@CS NC inhibits acid production by *S. mutans* at a lower concentration of CA. Not only that, CA@CS NC after 8 h will continue to slowly release CA to inhibit bacterial acid production.

In previous studies, it has been recognized that chitosan-based nanomaterials have reliable biosafety [19,57]. And CA@CS NC showed excellent biological safety in the results of CCK-8 cytotoxicity assay and HE staining tissue sections to detect the toxicity of CA@CS NC. Our studies proved that the CA

encapsulated chitosan-based nanocapsules not only did no obvious toxicity occur in the animal model, but greatly reduced the toxicity of CA *in vitro* by slow release without attenuating the antibacterial effect.

In our study, CA@CS NC downregulated the expression of *S. mutans* genes. Among them, *gtfB*, *gtfC*, and *gtfD* are related to extracellular polysaccharide synthesis, and down-regulation helps to inhibit biofilm formation. Downregulation of *VicR* and *gbpB* contributes to the inhibition of adhesion, biofilm formation, and virulence expression. In addition, *ComB*, *ComE*, *ComS*, *ComA*, and *ComR* are closely related to bacterial QS, and the down-regulation of these genes is of significance for inhibiting resistance. According to previous studies, QS allows bacterial groups to change behavior synchronously in response to changes in population density and species composition in nearby communities. *S. mutans* can use its multiple two-component QS system to resist the harsh physiological conditions of the oral environment and regulate the gene expression of multiple phenotypes [58,59]. Therefore, down-regulation of QS related genes is beneficial to interfere with the information exchange of *S. mutans*, regulate biofilm and virulence, and thus inhibit dental caries [60]. Alternatively, biofilm formation can protect bacteria from the action of antibiotics and is associated with bacterial resistance [61]. Biofilm formation is triggered by the bacterial QS system, and an extracellular matrix composed of polysaccharides, proteins, and extracellular DNA may prevent certain antibiotics from successfully penetrating the cell. Since QS induces deleterious properties such as biofilm formation or virulence, interfering with bacterial communication is a promising strategy to prevent the synchronization of bacterial virulence behavior [62]. In our study, CA@CS NC down-regulated QS gene, inhibited bacterial population effects such as biofilm formation and acid production, and better exerted the antibacterial effect of low-concentration CA.

Bacterial acid production, biofilm formation, and tooth demineralization and re-mineralization are the key factors in the process of caries formation [26,35]. On the one hand, plaque score can systematically quantify the number and distribution of bacteria on tooth surfaces after drug treatment. On the other hand, the Keyes scoring method is a systematic evaluation based on tooth structure, which can fully show the degree of tooth demineralization and the severity of lesions. In our results, plaque scores were significantly decreased after treatment with CA@CS NC. At the same time, the development of dental caries was inhibited in Keyes' scores results in CA@CS NC group. CA@CS NC shows similar

effects as NaF in a rat model, which provides a new idea for the future anti-biofilm and anti-caries treatment. Therefore, CA@CS NC may become a more suitable treatment option for patients with dental caries in high-fluoride areas. Keyes' scoring system is widely used in the quantitative evaluation of dental caries, which can evaluate the depth and number of dental caries by scores. In the process of dental caries, various cells and tissues in the dental pulp, including odontoblasts, fibroblasts, stem cells, immune cells, blood vessels and nerves, recognize pathogens early and participate in various inflammatory reactions, forming a variety of different defense mechanisms [63,64]. As secretory cells, odontoblasts have immune functions. And the products of microbial proliferation and metabolism can stimulate the surrounding dental pulp through the dentinal tubules and produce the effect of repairing dentine. Mild stimulation can up-regulate odontoblasts' activity to form reactionary dentine, while strong stimulation can cause their death and trigger a complex process involving the recruitment of dental pulp stem/progenitor cells to form reparative dentine [65]. According to previous studies, Wnt signaling and others induced this repair process, and the rat experiment showed a significant repair effect within 14 days [66,67]. In our animal results, there were no significant differences among groups for mild caries lesions (E). Based on the above theory, we speculate that the reparatory effect of odontoblasts makes the lesions that should be more severe still mild, and this effect is important for the rapid restoration of homeostasis so that the results are not different in superficial caries. In moderate and severe lesions (Ds, Dm, and Dx), the repair effect is not significant because of homeostatic imbalance caused by excessive stimulation. However, CA@CS NC inhibits the development of dental caries by virtue of its excellent antibacterial properties, and its effect is similar to that of clinical anti-caries drugs (NaF).

According to the existing results, CA@CS NC has reliable antibacterial and anti-caries performance, which is more effective than CA alone and less toxic (strictly, the performance is better *in vitro*, and there is no significant difference *in vivo*). CA@CS NC can adsorb the bacterial cell membrane through electrostatic interaction and target bacteria. By adding CA@CS NC to oral health preparations such as mouthwash and oral freshener, CA@CS NC can be combined with bacteria in the oral cavity through People's Daily mouth washing or brushing, which can inhibit bacteria and prevent dental caries. Compared with chlorhexidine and other oral bacteriostatic agents that have produced bacterial resistance, CA@CS NC can target bacteria and inhibit bacterial growth, acid production, biofilm formation and quorum sensing at a lower concentration. It is a new method for oral antibacterial and caries prevention.

As with all studies, this study has certain limitations. The occurrence and development of dental caries is a very complex problem, which is affected by multiple factors. At the same time, antibiotics must inevitably face the assessment of their effects on normal flora. At present, the establishment models for the study of microecology and drug evaluation are mainly divided into *in vivo* models and *in vitro* models. *In vitro* models often involve complex biofilms derived from a single bacterium, multiple species or even human saliva [68–70]. They have the advantage of having better control over experimental variables and producing more reproducible data, but do not well mimic the real situation *in vivo* [71]. According to previous studies, high-throughput sequencing of the 16 S rDNA gene may be more consistent with the real situation *in vitro* model [68]. On the other hand, Keyes' model is the main *in vivo* animal model used in studies, and the influence of saliva, chewing and eating is added. However, current *in vivo* models mainly rely on rodents, whose feeding patterns, saliva secretion and oral microecological structure are quite different from those of humans [72]. Nowadays, the human *in situ* model is considered as a method between *in vitro* and *in vivo* models, which can evaluate the real situation well and has great clinical value [73]. Nevertheless, human body model is complex and costly, and patient compliance has become a key factor for success [74]. According to the model above, choosing an appropriate model to analyze the effect of anticaries agents on the microbiota through genetic study is necessary in the future research.

In addition, the targeting effect of CA@CS NC is a relatively weak electrostatic force, which may also combine with other negatively potential enzymes and other substances in the oral cavity. And this targeting method of bacteria as a long-term treatment for dental caries depends on repeated multiple administrations. And people's chewing, swallowing and saliva can lead to its detachment from the teeth. While the bacteria are targeted by electrostatic forces in this study, further firm targeting of the tooth surface can further enhance its effect and reduce the dependence on repeated administration. If the chemical groups of CS are modified to prepare CS derivatives to target calcium ions and other dental targets, its dental targeting can be improved, which may be one of the future development directions [75].

Conclusion

We have developed CA@CS NC with an oil-based core and a positively potential CS shell, which are able to adsorb *S. mutans* through electrostatic interactions and slowly release CA, strongly inhibit bacterial growth, acid production, biofilm formation and QS, thereby showing effective and safe properties in

the prevention and treatment of biofilm. This strategy of chitosan-based nanocapsules for drug loading opens new avenues to improve the short duration of drug action and its application in antibacterial and antibiofilm drug development.

Disclosure statement

No potential conflict of interest was reported by the author(s).

Funding

This study was financially supported by the National Innovative Training Program for College Students [202110661044], the National Natural Science Foundation of China [32060227], Guizhou Provincial Natural Science Foundation [QKH-ZK[2021]Y114], Science and Technology Project of Guizhou Provincial Health Commission [gzwjkj2020-1-237], Zunyi Medical University 2018 Academic New Seedling Cultivation and Innovative Exploration Special Project [QKH[2018]5772-028], the future 'science and technology elite' project of Zunyi Medical University [ZYSE-2021-02], as well as the Innovative Training Program for College Students of Zunyi Medical University [ZHCX202001].

Author contributions

R.M. and X.Q. conceived the project and designed most of the experiments. Experiments were carried out by R.M., H. Z., X.L., Z.Z., J.J. and X.W. In addition, R.M., X.Q., H. Z. and Y.G. assisted in data analysis and discussion. R. M. wrote manuscripts. All the authors commented on the manuscript.

References

- [1] Selwitz RH, Ismail AI, Pitts NB. Dental caries. *Lancet* (London, England). 2007 Jan 6;369(9555):51–59. PubMed PMID: 17208642; eng. doi: [10.1016/s0140-6736\(07\)60031-2](https://doi.org/10.1016/s0140-6736(07)60031-2)
- [2] Hu C, Wang LL, Lin YQ, et al. Nanoparticles for the treatment of oral biofilms: current state, mechanisms, influencing factors, and prospects. *Adv Healthcare Mater*. 2019 Dec;8(24):e1901301. doi: [10.1002/adhm.201901301](https://doi.org/10.1002/adhm.201901301) PubMed PMID: 31763779; eng.
- [3] Bernabe E, Marcenes W, Hernandez CR, et al. Global, regional, and national levels and trends in burden of oral conditions from 1990 to 2017: a systematic analysis for the global burden of disease 2017 study. *J Dent Res*. 2020;99(4):362–373. doi: [10.1177/0022034520908533](https://doi.org/10.1177/0022034520908533)
- [4] James SL, Abate D, Abate KH. Global, regional, and national incidence, prevalence, and years lived with disability for 354 diseases and injuries for 195 countries and territories, 1990–2017: a systematic analysis for the Global Burden of Disease Study 2017. *The Lancet*. 2018 Nov 10;392(10159):1789–1858. PubMed PMID: 30496104; PubMed Central PMCID: PMC6227754. eng. doi: [10.1016/s0140-6736\(18\)32279-7](https://doi.org/10.1016/s0140-6736(18)32279-7)
- [5] Wen PYF, Chen MX, Zhong YJ, et al. Global burden and inequality of dental caries, 1990 to 2019. *J Dent Res*. 2022 Apr;101(4):392–399. doi: [10.1177/00220345211056247](https://doi.org/10.1177/00220345211056247) PubMed PMID: 34852668; eng.
- [6] Roncari Rocha G, Sims KR Jr., Xiao B, et al. Nanoparticle carrier co-delivery of complementary antibiofilm drugs abrogates dual species cariogenic biofilm formation in vitro. *J Oral Microbiol*. 2022;14(1):1997230. PubMed PMID: 34868474; PubMed Central PMCID: PMC6835615. eng. doi: [10.1080/20002297.2021.1997230](https://doi.org/10.1080/20002297.2021.1997230)
- [7] Bowen WH, Koo H. Biology of Streptococcus mutans-derived glucosyltransferases: role in extracellular matrix formation of cariogenic biofilms. *Caries Res*. 2011;45(1):69–86. doi: [10.1159/000324598](https://doi.org/10.1159/000324598) PubMed PMID: 21346355; PubMed Central PMCID: PMC63068567. eng.
- [8] Jakubovics NS, Goodman SD, Mashburn-Warren L, et al. The dental plaque biofilm matrix. *Periodontol* 2000. 2021 Jun;86(1):32–56. doi: [10.1111/prd.12361](https://doi.org/10.1111/prd.12361) PubMed PMID: 33690911; PubMed Central PMCID: PMC69413593. eng.
- [9] Valm AM. The structure of dental plaque microbial communities in the transition from health to dental caries and periodontal disease. *J Mol Biol*. 2019 Jul 26;431(16):2957–2969. PubMed PMID: 31103772; PubMed Central PMCID: PMC6646062. eng. doi: [10.1016/j.jmb.2019.05.016](https://doi.org/10.1016/j.jmb.2019.05.016)
- [10] Lamont RJ, Koo H, Hajishengallis G. The oral microbiota: dynamic communities and host interactions. *Nature Rev Microbiol*. 2018 Dec;16(12):745–759. PubMed PMID: 30301974; PubMed Central PMCID: PMC6278837. eng. doi: [10.1038/s41579-018-0089-x](https://doi.org/10.1038/s41579-018-0089-x)
- [11] Burgette JM, Dahl ZT, Yi JS, et al. Mothers' sources of child fluoride information and misinformation from social connections. *JAMA network open*. 2022 Apr 1;5(4):e226414. PubMed PMID: 35363267; PubMed Central PMCID: PMC68976236. eng. doi: [10.1001/jamanetworkopen.2022.6414](https://doi.org/10.1001/jamanetworkopen.2022.6414)
- [12] Whelton HP, Spencer AJ, Do LG, et al. Fluoride revolution and dental caries: evolution of policies for global use. *J Dent Res*. 2019 Jul;98(8):837–846. doi: [10.1177/0022034519843495](https://doi.org/10.1177/0022034519843495) PubMed PMID: 31282846; eng.
- [13] Balhaddad AA, Kansara AA, Hidan D, et al. Toward dental caries: exploring nanoparticle-based platforms and calcium phosphate compounds for dental restorative materials. *Bioact Mater*. 2019 Mar;4(1):43–55. PubMed PMID: 30582079; PubMed Central PMCID: PMC6299130. eng. doi: [10.1016/j.bioactmat.2018.12.002](https://doi.org/10.1016/j.bioactmat.2018.12.002)
- [14] Dutra-Correa M, Leite A, de Cara S, et al. Antibacterial effects and cytotoxicity of an adhesive containing low concentration of silver nanoparticles. *J Dent*. 2018 Oct;77:66–71. PubMed PMID: 30009857; eng. doi: [10.1016/j.jdent.2018.07.010](https://doi.org/10.1016/j.jdent.2018.07.010)
- [15] Andrade V, Martínez A, Rojas N, et al. Antibacterial activity against Streptococcus mutans and diametrical tensile strength of an interim cement modified with zinc oxide nanoparticles and terpenes: an in vitro study. *J Prosthet Dent*. 2018 May;119(5):e862.1–e862.7. doi: [10.1016/j.prosdent.2017.09.015](https://doi.org/10.1016/j.prosdent.2017.09.015) PubMed PMID: 29475754; eng.
- [16] Nizami MZI, VAW X, Yin IRX, et al. Metal and metal oxide nanoparticles in caries prevention: a review. *Nanomaterials*. 2021 Dec;11(12):3446. doi: [10.3390/](https://doi.org/10.3390/)

- nano11123446 PubMed PMID: WOS:000736183500001.
- [17] Benoit DSW, Sims KR, Jr., Fraser D. Nanoparticles for oral biofilm treatments. *ACS Nano*. 2019 May 28;13(5):4869–4875. PubMed PMID: 31033283; PubMed Central PMCID: PMC6707515. eng. doi: 10.1021/acsnano.9b02816
- [18] Song W, Ge S. Application of antimicrobial nanoparticles in dentistry. *Molecules (Basel, Switzerland)*. 2019 Mar 15;24(6):1033. PubMed PMID: 30875929; PubMed Central PMCID: PMC6470852. eng. doi: 10.3390/molecules24061033
- [19] Rashki S, Asgarpour K, Tarrahimofrad H, et al. Chitosan-based nanoparticles against bacterial infections. *Carbohydr Polym*. 2021 Jan 1;251:117108. PubMed PMID: 33142645; eng. doi: 10.1016/j.carbpol.2020.117108
- [20] Zhang C, Hui D, Du C, et al. Preparation and application of chitosan biomaterials in dentistry. *Int j biol macromol*. 2021 Jan 15;167:1198–1210. PubMed PMID: 33202273; eng. doi: 10.1016/j.ijbiomac.2020.11.073
- [21] Rizeq BR, Younes NN, Rasool K, et al. Synthesis, bioapplications, and toxicity evaluation of chitosan-based nanoparticles. *IJMS*. 2019 Nov 16;20(22):5776. PubMed PMID: 31744157; PubMed Central PMCID: PMC6688098. eng. doi:10.3390/ijms20225776
- [22] Gao H, Wu N, Wang N, et al. Chitosan-based therapeutic systems and their potentials in treatment of oral diseases. *Int j biol macromol*. 2022 Dec 1;222(Pt B):3178–3194. PubMed PMID: 36244538; eng. doi: 10.1016/j.ijbiomac.2022.10.090
- [23] Yanakiev S. Effects of cinnamon (*Cinnamomum* spp.) in dentistry: a review. *Molecules (Basel, Switzerland)*. 2020 Sep 12;25(18):4184. PubMed PMID: 32932678; PubMed Central PMCID: PMC7571082. eng. doi: 10.3390/molecules25184184
- [24] Cox HJ, Li J, Saini P, et al. Bioinspired and eco-friendly high efficacy cinnamaldehyde antibacterial surfaces. *J Mat Chem B*. 2021 Mar 28;9(12):2918–2930. PubMed PMID: 33885647; eng. doi: 10.1039/d0tb02379e
- [25] Sun J, Leng X, Zang J, et al. Bio-based antibacterial food packaging films and coatings containing cinnamaldehyde: A review. *Crit Rev Food Sci Nutr*. 2022 Jul 28;1–13. PubMed PMID: 35900224; eng. doi:10.1080/10408398.2022.2105300
- [26] He Z, Huang Z, Jiang W, et al. Antimicrobial activity of cinnamaldehyde on *Streptococcus mutans* biofilms. *Front Microbiol* [PubMed PMID: 31608045; PubMed Central PMCID: PMC6773874. eng]. 2019;10:2241. doi: 10.3389/fmicb.2019.02241
- [27] Kaiser M, Pereira S, Pohl L, et al. Chitosan encapsulation modulates the effect of capsaicin on the tight junctions of MDCK cells. *Sci Rep*. 2015 May 13;5(1):10048. PubMed PMID: 25970096; PubMed Central PMCID: PMC4429556. eng. doi:10.1038/srep10048
- [28] Qin X, Engwer C, Desai S, et al. An investigation of the interactions between an *E. coli* bacterial quorum sensing biosensor and chitosan-based nanocapsules. *Colloids Surf B Biointerfaces*. 2017 Jan 1;149:358–368. PubMed PMID: 27792985; eng. doi: 10.1016/j.colsurfb.2016.10.031
- [29] Sebelemetja M, Moeno S, Patel M. Anti-acidogenic, anti-biofilm and slow release properties of *Dodonaea viscosa* var. *angustifolia* flavone stabilized polymeric nanoparticles. *Arch Oral Biol*. 2020 Jan;109:104586. PubMed PMID: WOS:000523652700001. doi: 10.1016/j.archoralbio.2019.104586
- [30] Hasan S, Singh K, Danisuddin M, et al. Inhibition of major virulence pathways of *Streptococcus mutans* by quercitrin and deoxynojirimycin: a synergistic approach of infection control. *PLoS One*. 2014;9(3):e91736. PubMed PMID: 24622055; PubMed Central PMCID: PMC3951425. eng. doi: 10.1371/journal.pone.0091736
- [31] Kaur G, Balamurugan P, Princy SA. Inhibition of the Quorum sensing system (ComDE Pathway) by aromatic 1,3-di-m-tolylurea (DMTU): cariostatic effect with fluoride in Wistar rats. *Front cell infec microbiol*. 2017;7:313. PubMed PMID: 28748175; PubMed Central PMCID: PMC65506180. eng. doi: 10.3389/fcimb.2017.00313
- [32] Suzuki Y, Nagasawa R, Senpuku H. Inhibiting effects of fructanase on competence-stimulating peptide-dependent quorum sensing system in *Streptococcus mutans*. *J Infect Chemother*. 2017 Sep;23(9):634–641. PubMed PMID: 28729051; eng. doi: 10.1016/j.jiac.2017.06.006
- [33] Ham S-Y, Kim H-S, Cha E, et al. Raffinose inhibits *Streptococcus mutans* biofilm formation by targeting glucosyltransferase. *Microbiol Spectr*. 2022;10(3):e02076–21. doi: 10.1128/spectrum.02076-21
- [34] Wang Y, Zeng Y, Wang Y, et al. Antimicrobial peptide GH12 targets *Streptococcus mutans* to arrest caries development in rats. *J Oral Microbiol*. 2019;11(1):1549921. doi: 10.1080/20002297.2018.1549921
- [35] Jiang W, Wang Y, Luo J, et al. Antimicrobial peptide GH12 prevents dental caries by regulating dental plaque microbiota. *Appl environ microbiol*. 2020 Jul 2;86(14):PubMed PMID: 32414800; PubMed Central PMCID: PMC7357485. eng. doi:10.1128/aem.00527-20
- [36] Arifin WN, Zahiruddin WM. Sample size calculation in animal studies using resource equation approach. *Malays J Med Sci*. 2017 Oct;24(5):101–105. PubMed PMID: 29386977; PubMed Central PMCID: PMC65772820. eng. doi: 10.21315/mjms2017.24.5.11
- [37] Tian MJ, Wang W, Fan MZ, et al. Effect of Se-enriched *Pleurotus ostreatus* on organ index and anti-oxidative capability of rats. *Chin J Microecol*. 2010;22(11):1001–1003+1007. doi: 10.13381/j.cnki.cjm.2010.11.005
- [38] Zhou Q, Zhu J, Liu B, et al. Effects of high-dose of copper amino acid complex on laying performance, hematological and biochemical parameters, organ index, and histopathology in laying hens. *Biol Trace Element Res*. 2021 Aug;199(8):3045–3052. doi: 10.1007/s12011-020-02406-2 PubMed PMID: 33044710; eng.
- [39] Naka S, Wato K, Misaki T, et al. *Streptococcus mutans* induces IgA nephropathy-like glomerulonephritis in rats with severe dental caries. *Sci Rep*. 2021 Mar 11;11(1):5784. PubMed PMID: 33707585; PubMed Central PMCID: PMC67952735. eng. doi:10.1038/s41598-021-85196-4
- [40] Keyes PH. Dental caries in the molar teeth of rats. II. A method for diagnosing and scoring several types of lesions simultaneously. *J Dent Res*. 1958 Nov-Dec;37(6):1088–1099. PubMed PMID: 13611123; eng. doi: 10.1177/00220345580370060901

- [41] Keyes PH. Dental caries in the molar teeth of rats. I. Distribution of lesions induced by high-carbohydrate low-fat diets. *J Dent Res.* 1958 Nov-Dec;37(6):1077–1087. PubMed PMID: 13611122; eng. doi: [10.1177/00220345580370060801](https://doi.org/10.1177/00220345580370060801)
- [42] MDJAM H. Measurement of crystal size distributions. *Am Mineralog.* 2000;85(9):1105–1116. doi: [10.2138/am-2000-8-901](https://doi.org/10.2138/am-2000-8-901)
- [43] Hao X, Chen S, Qin D, et al. Antifouling and antibacterial behaviors of capsaicin-based pH responsive smart coatings in marine environments. *Mater Sci Eng C.* 2020 Mar;108:110361. PubMed PMID: 31923998; eng. doi: [10.1016/j.msec.2019.110361](https://doi.org/10.1016/j.msec.2019.110361)
- [44] Fernández-Paz E, Feijoo-Siota L, Gaspar MM, et al. Microencapsulated chitosan-based nanocapsules: a new platform for pulmonary gene delivery. *Pharmaceutics.* 2021 Aug 31;13(9):1377. PubMed PMID: 34575452; PubMed Central PMCID: PMCPCMC8472419. eng. doi:[10.3390/pharmaceutics13091377](https://doi.org/10.3390/pharmaceutics13091377)
- [45] Khattak S, Wahid F, Liu LP, et al. Applications of cellulose and chitin/chitosan derivatives and composites as antibacterial materials: current state and perspectives. *Appl Microbiol Biotechnol.* 2019 Mar;103(5):1989–2006. doi: [10.1007/s00253-018-09602-0](https://doi.org/10.1007/s00253-018-09602-0) PubMed PMID: 30637497; eng.
- [46] Wang W, Meng Q, Li Q, et al. Chitosan derivatives and their application in biomedicine. *IJMS.* 2020 Jan 12;21(2):487. PubMed PMID: 31940963; PubMed Central PMCID: PMCPCMC7014278. eng. doi:[10.3390/ijms21020487](https://doi.org/10.3390/ijms21020487)
- [47] Vasiliu S, Racovita S, Gugoasa IA, et al. The benefits of smart nanoparticles in dental applications. *Int J Mol Sci.* 2021 Mar;22(5):2585. doi: [10.3390/ijms22052585](https://doi.org/10.3390/ijms22052585) PubMed PMID: WOS:000628313000001.
- [48] Belbekhouche S, Bousserhine N, Alphonse V, et al. Chitosan based self-assembled nanocapsules as antibacterial agent. *Colloids Surf B Biointerfaces.* 2019 Sep;181:158–165. PubMed PMID: WOS:000481565300021. doi: [10.1016/j.colsurfb.2019.05.028](https://doi.org/10.1016/j.colsurfb.2019.05.028)
- [49] Shoueir KR, El-Desouky N, Rashad MM, et al. Chitosan based-nanoparticles and nanocapsules: overview, physicochemical features, applications of a nanofibrous scaffold, and bioprinting. *Int j biol macromol.* 2021 Jan;167:1176–1197. PubMed PMID: WOS:000606683200104. doi: [10.1016/j.ijbiomac.2020.11.072](https://doi.org/10.1016/j.ijbiomac.2020.11.072)
- [50] Bai YT, Wang TR, Zhang SL, et al. Recent advances in organic and polymeric carriers for local tumor chemo-immunotherapy. *Sci China Technol Sci.* 2022 May;65(5):1011–1028. doi: [10.1007/s11431-021-1961-y](https://doi.org/10.1007/s11431-021-1961-y) PubMed PMID: WOS:000782192700001.
- [51] Wang WH, Hao XP, Chen SG, et al. Ph-responsive Capsaicin@chitosan nanocapsules for antibiofouling in marine applications. *Polymer.* 2018 Dec;158:223–230. PubMed PMID: WOS:000450910100027. doi: [10.1016/j.polymer.2018.10.067](https://doi.org/10.1016/j.polymer.2018.10.067)
- [52] Wang L, Zhu SX, Zou CP, et al. Preparation and evaluation of the anti-cancer properties of RGD-modified curcumin-loaded chitosan/perfluorohexane nanocapsules in vitro. *Heliyon.* 2022 Jul;8(7):e09931. doi: [10.1016/j.heliyon.2022.e09931](https://doi.org/10.1016/j.heliyon.2022.e09931) PubMed PMID: WOS:000843671700018.
- [53] Choukaife H, Seyam S, Alallam B, et al. Current advances in chitosan nanoparticles based oral drug delivery for colorectal cancer treatment. *Int J Nanomed [PubMed PMID: WOS:000863243200001].* 2022;17:3933–3966. doi: [10.2147/ijn.S375229](https://doi.org/10.2147/ijn.S375229)
- [54] Chen XQ, Daliri EBM, Tyagi A, et al. Cariogenic biofilm: pathology-related phenotypes and targeted therapy. *Microorganisms.* 2021 Jun;9(6):1311. doi: [10.3390/microorganisms9061311](https://doi.org/10.3390/microorganisms9061311) PubMed PMID: WOS:000665986000001.
- [55] Lin YW, Zhou XD, Li YQ. Strategies for Streptococcus mutans biofilm dispersal through extracellular polymeric substances disruption. *Mol Oral Microbiol.* 2022 Feb;37(1):1–8. PubMed PMID: WOS:000721482800001. doi: [10.1111/omi.12355](https://doi.org/10.1111/omi.12355)
- [56] Wright PP, Ramachandra SS. Quorum sensing and quorum quenching with a focus on cariogenic and periodontopathic oral Biofilms. *Microorganisms.* 2022 Sep;10(9):1783. PubMed PMID: WOS:000857549700001. doi: [10.3390/microorganisms10091783](https://doi.org/10.3390/microorganisms10091783)
- [57] Fakhri E, Eslami H, Maroufi P, et al. Chitosan biomaterials application in dentistry. *Int j biol macromol.* 2020 Nov 1;162:956–974. PubMed PMID: 32599234; eng. doi: [10.1016/j.ijbiomac.2020.06.211](https://doi.org/10.1016/j.ijbiomac.2020.06.211)
- [58] Lemos JA, Burne RA. A model of efficiency: stress tolerance by Streptococcus mutans. *Microbiology (Reading England).* 2008 Nov;154(Pt 11):3247–3255. PubMed PMID: 18957579; PubMed Central PMCID: PMCPCMC2627771. eng. doi: [10.1099/mic.0.2008/023770-0](https://doi.org/10.1099/mic.0.2008/023770-0)
- [59] Smith EG, Spatafora GA. Gene regulation in S. mutans: complex control in a complex environment. *J Dent Res.* 2012 Feb;91(2):133–141. PubMed PMID: 21743034; eng. doi: [10.1177/00220345111415415](https://doi.org/10.1177/00220345111415415)
- [60] Leung V, Dufour D, Lévesque CM. Death and survival in Streptococcus mutans: differing outcomes of a quorum-sensing signaling peptide. *Front Microbiol.* 2015;6:1176. PubMed PMID: 26557114; PubMed Central PMCID: PMCPCMC4615949. eng. doi: [10.3389/fmicb.2015.011176](https://doi.org/10.3389/fmicb.2015.011176)
- [61] Baptista PV, McCusker MP, Carvalho A, et al. Nanostrategies to fight multidrug resistant bacteria-“a battle of the titans”. *Front Microbiol [PubMed PMID: 30013539; PubMed Central PMCID: PMCPCMC6036605. eng].* 2018;9:1441. doi: [10.3389/fmicb.2018.01441](https://doi.org/10.3389/fmicb.2018.01441)
- [62] Rémy B, Mion S, Plener L, et al. Interference in bacterial quorum sensing: a biopharmaceutical perspective. *Front Pharmacol [PubMed PMID: 29563876; PubMed Central PMCID: PMCPCMC5845960. eng].* 2018;9:203. doi: [10.3389/fphar.2018.00203](https://doi.org/10.3389/fphar.2018.00203)
- [63] Galler KM, Weber M, Korkmaz Y, et al. Inflammatory response mechanisms of the dentine-pulp complex and the periapical tissues. *IJMS.* 2021 Feb 2;22(3):1480. PubMed PMID: 33540711; PubMed Central PMCID: PMCPCMC7867227. eng. doi:[10.3390/ijms22031480](https://doi.org/10.3390/ijms22031480)
- [64] Farges JC, Alliot-Licht B, Renard E, et al. Dental pulp defence and repair mechanisms in dental caries. *Mediators Inflamm [PubMed PMID: 26538821; PubMed Central PMCID: PMCPCMC4619960. eng].* 2015;2015:1–16. doi: [10.1155/2015/230251](https://doi.org/10.1155/2015/230251)
- [65] Bjørndal L, Simon S, Tomson PL, et al. Management of deep caries and the exposed pulp. *Int Endod J.* 2019 Jul;52(7):949–973. doi: [10.1111/iej.13128](https://doi.org/10.1111/iej.13128) PubMed PMID: 30985944; eng.
- [66] Florimond M, Minic S, Sharpe P, et al. Modulators of Wnt signaling pathway implied in dentin pulp complex engineering: a literature review. *IJMS.* 2022 Sep 13;23(18):10582. PubMed PMID: 36142496; PubMed

- Central PMCID: PMCPMC9502831. eng. doi:[10.3390/ijms231810582](https://doi.org/10.3390/ijms231810582)
- [67] Hunter DJ, Bardet C, Mouraret S, et al. Wnt acts as a prosurvival signal to enhance dentin regeneration. *J Bone Miner Res.* **2015** Jul;30(7):1150–1159. doi: [10.1002/jbmr.2444](https://doi.org/10.1002/jbmr.2444) PubMed PMID: 25556760; eng.
- [68] Hu J, Yu J, Liu H, et al. Dynamic killing effectiveness of mouthrinses and a d-enantiomeric peptide on oral multispecies biofilms grown on dental restorative material surfaces. *J Dent.* **2023** May 16;134:104552. PubMed PMID: 37201774; eng. doi: [10.1016/j.jdent.2023.104552](https://doi.org/10.1016/j.jdent.2023.104552)
- [69] Jiang W, Xie Z, Huang S, et al. Targeting cariogenic pathogens and promoting competitiveness of commensal bacteria with a novel Ph-responsive antimicrobial peptide. *J Oral Microbiol.* **2023**;15(1):2159375. PubMed PMID: 36570976; PubMed Central PMCID: PMCPMC9788686. eng. doi: [10.1080/20002297.2022.2159375](https://doi.org/10.1080/20002297.2022.2159375)
- [70] Wu Y, Gao H, Liu J, et al. Chitosan nanoparticles efficiently enhance the dispersibility, stability and selective antibacterial activity of insoluble isoflavonoids. *Int J Biol Macromol.* **2023** Mar 31;232:123420. PubMed PMID: 36708890; eng. doi: [10.1016/j.ijbiomac.2023.123420](https://doi.org/10.1016/j.ijbiomac.2023.123420)
- [71] Zhou W, Peng X, Zhou X, et al. Novel nanocomposite inhibiting caries at the enamel restoration margins in an in vitro saliva-derived biofilm secondary caries model. *IJMS.* **2020** Sep 2;21(17):6369. PubMed PMID: 32887330; PubMed Central PMCID: PMCPMC7503730. eng. doi:[10.3390/ijms21176369](https://doi.org/10.3390/ijms21176369)
- [72] Zhou W, Chen H, Weir MD, et al. Novel bioactive dental restorations to inhibit secondary caries in enamel and dentin under oral biofilms. *J Dent.* **2023** Jun;133:104497. PubMed PMID: 37011782; eng. doi: [10.1016/j.jdent.2023.104497](https://doi.org/10.1016/j.jdent.2023.104497)
- [73] Paradella TC, Koga-Ito CY, Jorge AO. Ability of different restorative materials to prevent in situ secondary caries: analysis by polarized light-microscopy and energy-dispersive X-ray. *Eur J Oral Sci.* **2008** Aug;116(4):375–380. PubMed PMID: 18705806; eng. doi: [10.1111/j.1600-0722.2008.00544.x](https://doi.org/10.1111/j.1600-0722.2008.00544.x)
- [74] Ferracane JL. Models of caries formation around dental composite restorations. *J Dent Res.* **2017** Apr;96(4):364–371. PubMed PMID: 28318391; PubMed Central PMCID: PMCPMC5384487. eng. doi: [10.1177/0022034516683395](https://doi.org/10.1177/0022034516683395)
- [75] Kang M, Kim S, Kim H, et al. Calcium-binding polymer-coated poly(lactide- co-glycolide) microparticles for sustained release of quorum sensing inhibitors to prevent biofilm formation on hydroxyapatite surfaces. *ACS Appl Mater Inter.* **2019** Feb 27;11(8):7686–7694. PubMed PMID: 30768237; eng. doi: [10.1021/acsami.8b18301](https://doi.org/10.1021/acsami.8b18301)